

T. FRĄCZEK,\* M. OLEJNIK\*, M. PILARSKA\*,#

**X-RAY PHASE ANALYSIS OF NITRIDED LAYERS OF X2CrNiMo17-12-2 AUSTENITIC STEEL****RENTGENOWSKA ANALIZA FAZOWA WARSTW AZOTOWANYCH STALI AUSTENITYCZNEJ X2CrNiMo17-12-2**

This work presents the results of diffraction analyses carried out using X-ray phase analyses (XRD and GIXRD) of nitrided layers of X2CrNiMo17-12-2 austenitic steel. Plasma nitriding process was carried out in the temperature range of 325  $\div$  400 °C and time of 2  $\div$  4 h. Hydrogen-nitrogen plasma was used as reactive atmosphere (H<sub>2</sub> 75% + N<sub>2</sub> 25%) with pressure of 150 Pa. On the basis of the X-ray analyses it was stated that the obtained nitrided layers consisted of a subsurface layer of chromium nitrides and a zone of nitrogen saturated austenite.

W pracy zaprezentowano wyniki badań strukturalnych metodą rentgenowską analizy fazowej (XRD i GIXRD) warstw azotowanych na podłożu stali austenitycznej X2CrNiMo17-12-2. Proces azotowania jarzeniowego przeprowadzono w zakresie temperatur 325  $\div$  400 °C i czasu 2  $\div$  4 h. Atmosferę reaktywną stanowiła plazma wodorowo-azotowa (H<sub>2</sub> 75% + N<sub>2</sub> 25%) o ciśnieniu 150 Pa. Na podstawie badań rentgenowskich stwierdzono, że otrzymane warstwy azotowane składają się z przypowierzchniowej warstwy azotków chromu oraz strefy austenitu przesyczonego azotem. Zastosowanie ekranu aktywnego spowodowało wzrost głębokości dyfuzji azotu w głąb azotowanej powierzchni oraz zwiększyło jego koncentrację w fazie austenitu przesyczonego azotem.

**1. Introduction**

Modern advantage of constructions and technology determines the necessity to use materials with much better mechanical and performance properties. As a result, thermal and chemical treatment technologies are used in designing and manufacturing of engineering materials with established performance properties [1]. Plasma nitriding processes are used in order to guarantee optimal hardness of a metal surface, especially of stainless steel, its abrasion and corrosion resistance [2]. However, nitriding of high chromium steel faces a lot of difficulties due to a hermetic layer of chromium oxides, which make the process of nitriding more difficult or even impossible. In practice, this difficulty is overcome by an initial surface treatment, such as pickling and phosphate coating, or by introducing such additives as ammonium chloride or HCl to the reactive chamber, or by using plasma treatment or using combination of initial ion sputtering in the conditions of glow discharge and the following gas nitriding [3].

The most important factor in X-ray diffraction analysis which influences the precision of measurement is the depth of X-rays penetration of a given wavelength and obtaining information from a certain depth of the material. The depth

of X-rays penetration has an important role in examination of layers and coatings [4, 5].

As a result of nitriding the obtained nitrided layers of a shallow depth are characterized by zone structure and a sudden decrease of nitrogen concentration as a distance from the surface of the material increases.

**2. Material and testing methodology**

X2CrNiMo17-12-2 austenitic steel was subjected to the process of plasma nitriding according to PN-EN 10088-1:1998 (316L according to AISI), its chemical composition is presented in Table 1.

The process of plasma nitriding was carried out on a plasma treatment bench with a cooling anode type JON-600 powered by an impulse electric power supply Dora Power System MSS-10. In order to intensify the plasma nitriding process, an active cylindrical screen was placed on the cathode ( $\varnothing 200 \times 100$  mm) made of perforated sheet, its chemical composition is similar to the nitrided element - X5CrNi18-10 austenitic steel.

The parameters of the nitriding process were determined according to the scheme presented in Figure 1. The range of

\* CZĘSTOCHOWA UNIVERSITY OF TECHNOLOGY, FACULTY OF PRODUCTION ENGINEERING AND MATERIALS TECHNOLOGY, 19 ARMII KRAJOWEJ AV., 42-201 CZĘSTOCHOWA, POLAND

# Corresponding author: mpilarska@wip.pcz.pl

TABLE 1

Chemical composition of X2CrNiMo17-12-2 nitrided steel

| Element | C   | Cr   | Ni    | Mo    | Mn   | N    | Si   | P    | S     | Cu    | Fe       |
|---------|-----|------|-------|-------|------|------|------|------|-------|-------|----------|
| 1       | min | -    | 16.0  | 10.0  | 2.0  | -    | -    | -    | -     | -     | the rest |
|         | max | 0.03 | 18.0  | 14.0  | 3.0  | 2.0  | 0.11 | 1.0  | 0.045 | 0.03  |          |
| 2       | =   | 0.02 | 16.82 | 10.07 | 2.07 | 1.58 | 0.06 | 0.52 | 0.028 | 0.029 | 0.88     |

1 – chemical composition according to PN-EN 10088-1:1998  
2 – chemical composition of nitrided steel – according to the MEST 451139/2007 certificate

temperatures and times of nitriding was assumed on the basis of the carried out initial research concerning short-term and low-temperature plasma nitriding of austenitic steels [6]. The main criterion determining selection of nitriding parameters was obtainment of nitrided layers of given performance properties and maintaining good corrosion resistance of the nitrided austenitic steel.

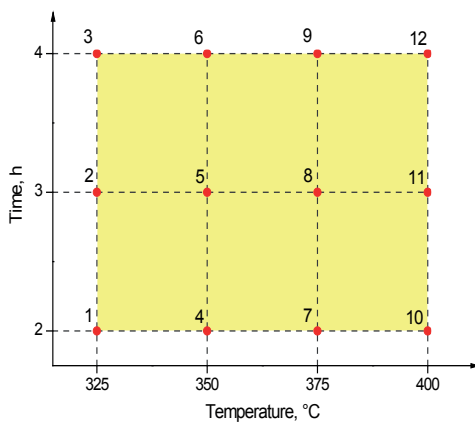


Fig. 1. Scheme of research

Plasma nitriding processes of X2CrNiMo17-12-2 austenitic steel were carried out in the temperature range of 325–400 °C and time of 2–4 h. After initial activation of the specimen's surface with argon ions, hydrogen-nitrogen plasma (H<sub>2</sub> 75%, N<sub>2</sub> 25%) was used, its pressure was 150 Pa. The voltage generating glow discharge during nitriding was 880–935 V, and during the stage of cathode sputtering it was almost 935 V.

The specimens were placed in a discharge chamber in two ways:

- directly on the cathode,
- on the cathode under an active screen.

The X-ray analyses were carried out using Seifert 3003TT X-ray diffractometer. In the experiment radiation coming from a cobalt anode X-ray tube was used; it emits radiation of wavelength  $\lambda_{\text{Co}} = 0.1789 \text{ nm}$ . During the analyses the voltage powering the tube was 30 kV. However, the current in the tube's network was 40 mA. The X-ray analyses included Bragg-Brentano XRD measurements and grazing incidence X-ray diffraction analysis (GIXRD). The XRD analyses, which are used for general identification of the phases occurring

in nitrided surface layers, were carried out in the range of diffraction angles  $2\Theta = 20^\circ \div 125^\circ$  with an angle step  $0.1^\circ$ ; the time of X-ray exposition was 4 s. The GIXRD measurements, which were carried out in order to obtain information about the zone phase structure of the analyzed nitrided layers from a particular depth, were made in a smaller range of diffraction angles ( $2\Theta = 35^\circ \div 75^\circ$ ), including reflections mainly from austenite and nitride phases. The XRD analyses were carried out at the angles of X-ray penetration  $\alpha = 1.5^\circ; 3^\circ; 5^\circ; 7^\circ; 9^\circ; 12^\circ$ . The obtained diffraction patterns were approximated by pseudo-Voigt function in order to determine the location of the diffraction reflections with the help of Analyze software.

### 3. Results and discussion

#### Determination X-rays penetration depth

X-ray analyses do not give a possibility to determine from which depth the obtained information comes. It is possible, however, to determine a part of total grazing incident  $G_x$  which comes from the subsurface layer at the depth  $x$  [7]. In the GIXRD method, the  $x$  value is determined from the formula (1):

$$x = \frac{-h(1 - G_x)}{\mu \left( \frac{1}{\sin \alpha} + \frac{1}{\sin(2\Theta - \alpha)} \right)} \quad (1)$$

The value of linear adsorption coefficient ( $\mu$ ) of the examined nitrided layers was determined according to a modified equation (2) presented in work [8] on the basis of data shown in Table 2:

$$\mu = \sum_{i=1}^n \left( \frac{\mu}{\rho} \right)_i m_i \rho_{316L} \quad (2)$$

where:  $\mu/\rho$  – mass adsorption coefficient,  $\text{cm}^2/\text{g}$ ;  $m_i$  – weight fraction of particular elements;  $\rho$  – density,  $\text{g}/\text{cm}^3$  (8 g/ $\text{cm}^3$  for X2CrNiMo17-12-2 steel).

Weight fractions of particular elements were determined for the surface layer obtained on the X2CrNiMo17-12-2 cathodic nitrided steel, at parameters 400°C / 3 h, on the basis of average value of the elements concentration at the depth of 10 μm (Table 2). Atomic fractions were determined by a method of linear analysis of chemical composition using glow discharge optical emission spectroscopy (GDOES).

TABLE 2  
Average chemical composition of the nitrided layer and values of mass absorption coefficients of particular elements

| #  | Element | Mass concentration, % | Mass absorption coefficient*, cm <sup>2</sup> /g |
|----|---------|-----------------------|--|
| 1  | Fe      | 67.96                 | 59.5   |
| 2  | Cr      | 15.46                 | 392  |
| 3  | Ni      | 9.12                  | 75.1   |
| 4  | Mo      | 4.19                  | 242  |
| 5  | Mn      | 2.05                  | 431  |
| 6  | Si      | 0.31                  | 94.1   |
| 7  | Cu      | 0.57                  | 79.8   |
| 8  | N       | 0.30                  | 13.6   |
| 9  | C       | 0.02                  | 8.5  |
| 10 | P       | 0.01                  | 113  |
| 11 | S       | 0.02                  | 153  |

\*Co K $\alpha$   $\lambda = 0.1789$  nm

Linear distribution of mass concentration of elements for the analyzed layer is presented in Figure 2.

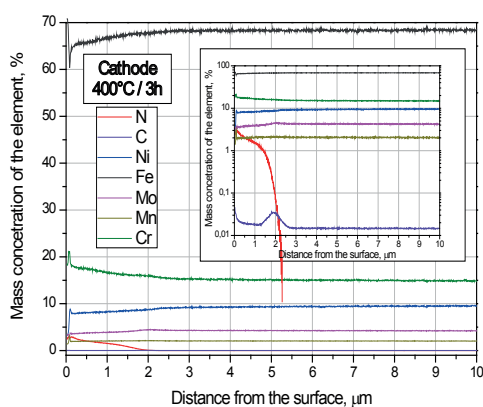


Fig. 2. Linear distribution of elements concentration for the cathode-nitrided layer (400°C / 3 h – GDOES)

Table 3 presents the depths of X-rays penetration, depending on the assumed total fraction of grazing incident coming from the subsurface layer at a given depth ( $G_x$ ), which were calculated for radiation coming from a cobalt anode tube which emits radiation of wavelength  $\lambda C_o = 0.1789$  nm and the analyzed material with a calculated linear adsorption coefficient  $\mu = 1021$  cm<sup>-1</sup>. The calculations were carried out for a diffraction angle  $2\Theta = 51^\circ$  which approximately corresponds to a main peak of austenite.

TABLE 3

Depth of X-rays penetration (μm) in the GIXRD method

| Angle $\alpha$ , ° | G <sub>x</sub> , % - the GIXRD method |      |      |      |      |      |      |
|--------------------|---------------------------------------|------|------|------|------|------|------|
|                    | 25                                    | 50   | 66   | 85   | 90   | 95   | 99   |
| 1.5                | 0.07                                  | 0.17 | 0.27 | 0.47 | 0.57 | 0.75 | 1.15 |
| 3                  | 0.14                                  | 0.34 | 0.52 | 0.91 | 1.12 | 1.46 | 2.24 |
| 5                  | 0.23                                  | 0.54 | 0.85 | 1.44 | 1.81 | 2.35 | 3.61 |

|    |      |      |      |      |      |      |      |
|----|------|------|------|------|------|------|------|
| 7  | 0.31 | 0.74 | 1.15 | 1.93 | 2.45 | 3.17 | 4.90 |
| 9  | 0.38 | 0.92 | 1.43 | 2.35 | 3.05 | 3.97 | 6.10 |
| 12 | 0.48 | 1.17 | 1.82 | 2.90 | 3.88 | 5.05 | 7.76 |

for:  $2\Theta=51^\circ$  and  $\mu=1021.4$  cm<sup>-1</sup>

The boundary value  $G_x$ , from which useful information was gathered, was assumed to be 85%. This value was determined on the basis of comparing X-ray analyses and linear analyses of chemical composition of the layers by the GDOES method.

On the basis of calculations of X-rays penetration depth for parameter  $G_x$ , which is 85%, it is possible to state that during the X-ray analyses carried out by GIXRD method (Table 3) theoretical depth, from which useful information comes from, for the angle  $\alpha = 12^\circ$ , will be about 3 μm. Regarding the obtained depths of nitrogen diffusion for the cathode-nitrided samples (max. 2.51 μm) this value exceeds the depth of the obtained nitrided layers. Thus, the GIXRD analyses could be finished at lower angles  $\alpha$ , which will significantly limit the time of measuring. Practically, for all the samples nitrided with the use of an active screen in temperature 350°C and more, maximal angle  $\alpha = 12^\circ$  can be insufficient to obtain information from the deepest zones of the obtained nirtidied layers. For this variant of the process the thickness of the obtained nitrided values (max. 6.34 μm) in most cases is higher than the calculated depth of X-rays penetration.

TABLE 4  
Depth of X-rays penetration (μm) in XRD method

| Angle 2 $\Theta$ , ° | G <sub>x</sub> , % - Bragg-Brentano XRD method |      |      |      |      |      |      |
|----------------------|--|------|------|------|------|------|------|
|                      | 25   | 50   | 66   | 85   | 90   | 95   | 99   |
| 30                   | 0.36   | 0.88 | 1.37 | 2.40 | 2.92 | 3.80 | 5.83 |
| 40                   | 0.48   | 1.16 | 1.81 | 3.18 | 3.38 | 5.02 | 7.71 |
| 50                   | 0.60   | 1.43 | 2.23 | 3.92 | 4.76 | 6.20 | 9.53 |
| 60                   | 0.70   | 1.70 | 2.64 | 4.64 | 5.64 | 7.33 | 11.3 |
| 70                   | 0.81   | 1.95 | 3.03 | 5.33 | 6.46 | 8.41 | 12.9 |
| 80                   | 0.91   | 2.18 | 3.39 | 5.97 | 7.24 | 9.43 | 14.5 |

$\mu=1021.4$  cm<sup>-1</sup>

Theoretically calculated depth of X-rays penetration for  $G_x = 85\%$  in typical XRD analyses (Table 4), in the range of diffraction angles 2 $\Theta$  corresponding to main reflections from the phases ( $40 \div 60^\circ$ ) is greater than the depth of the majority of the obtained nitrided layers. That is why, it is possible to notice distinct peaks coming from the austenitic base on the diffraction patterns. Only for the layers nitrided in temperature 400 °C with the use of an active screen, the depth of the obtained subsurface layers is bigger or equal to the boundary depth of X-rays penetration. In this case, reflections coming from the base will probably be small or will not appear on diffraction patterns.

#### X-ray diffraction measurements - XRD

The diffraction patterns obtained in XDR measurements of X2CrNiMo17-12-2 austenitic steel as delivered and after different variants of plasma nitriding are shown in Figure 3.

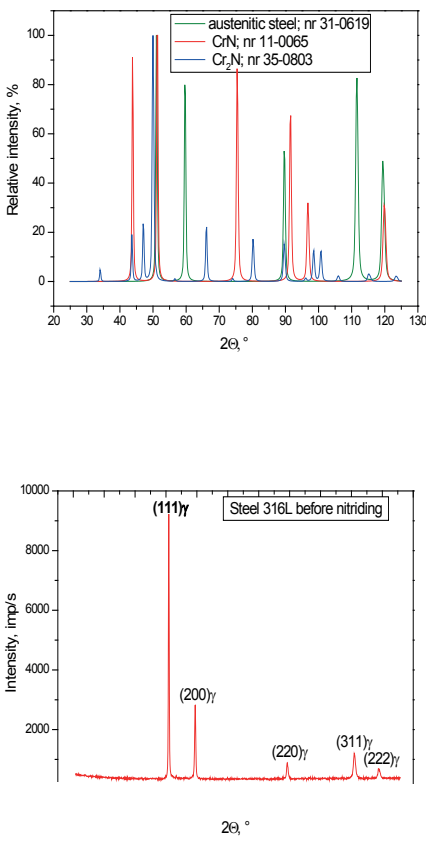


Fig. 3. Standard diffraction patterns of X2CrNiMo17-12-2 austenitic steel

On the diffraction pattern obtained from austenitic steel as delivered only reflections coming from austenite are visible. After plasma nitriding processes of X2CrNiMo17-12-2 steel on diffraction areas (Fig. 4) there are also reflections coming from nitrides CrN and Cr<sub>2</sub>N, as well as from nitrogen saturated austenite γ<sub>N</sub>. Increasing the time and temperature of nitriding caused an increase of percentage of nitrides and nitrogen saturated austenite in the upper layer. However, not only temperature and time but also configuration of the process, that is the use of an active screen, has an influence on the increase of percentage of these phases which significantly increase effects of nitriding.

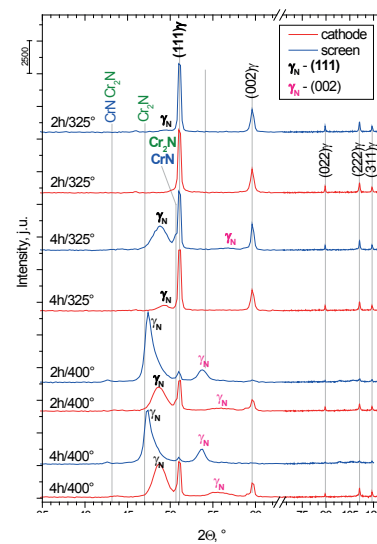


Fig. 4. Diffraction patterns of X2CrNiMo17-12-2 steel after different variants of plasma nitriding

#### Grazing incident X-ray diffraction analyses - GIXRD

The GIXRD analyses were carried out for angles of incidence of x-rays  $\alpha = 1,5; 3; 5; 7; 9; 12^\circ$ . In order to illustrate phase structure of the obtained nitrided layers, both diffraction images obtained by GIXRD method and results of XRD analyses of the same surface were presented. It was assumed that total percentage of grazing incident coming from the subsurface layer at a given depth ( $G_x$ ) was 85%.

Diffraction patterns of the samples nitrided with the use of an active screen in temperature of 400°C and time of 4 h and 2 h look similar (Fig. 5a, 7a). Diffractions performed at angles of incidence of X-rays  $\alpha = 1,5; 3; 5; 7; 9^\circ$  represent the nitrided layer. These diffraction patterns show peaks coming from chromium nitrides (CrN and Cr<sub>2</sub>N) and nitrogen saturated austenite. Diffraction analyses carried out at the smallest angles of incidence  $\alpha$  (1,5; 3°) confirm that closer to the surface both nitrogen saturated austenite and nitrides occur. Intensity of the peaks coming from the nitrogen saturated austenite increases when the angle of incidence of X-rays grows, because it is more possible to obtain information from greater depths. It means that in deeper areas of the obtained nitrided layers there is nitrogen saturated austenite which is free from nitride phase precipitations. In diffraction patterns made at  $\alpha = 12^\circ$  there was a peak from the base. On the basis of the obtained results and calculations of the depth of X-rays penetration we can state that the nitrided layers have an estimated depth on the level of 3 μm (Fig. 5a and 7a).

In the case of diffraction patterns obtained from the cathode-nitrided samples at process parameters of 400 °C and time of 4 h and 2 h, the situation is similar (Fig. 6a and 8a). This method did not show significant differences in depths of the nitrided layers when the time of nitriding increases from 2 to 4 hours. This layer is, however, thinner than in the case of nitriding with the use of an active screen. When the angle of incidence is  $\alpha = 7^\circ$  (which corresponds to

the depth of  $\mu\text{m}$ ) information comes from the nitrided layers only. These layers, similar to the other layers discussed in this work, are characterized by a zone structure. In the subsurface area there are peaks from both chromium nitrides and nitrogen saturated austenite. When the angle of incidence of X-ray increases, the intensity of reflection from nitrogen saturated austenite grows, which means that the amount of this phase at greater depths increases at the expense of the amount of nitrides phases. When  $\alpha = 9$  and  $12^\circ$ , the obtained information also comes from the base, which means that the cathode-nitrided layer has an estimated depth of  $2 \mu\text{m}$ , it is 30% less than from nitriding at the same parameters but with the use of an active screen.

The layer nitrided with the use of an active screen at temperature of  $325^\circ\text{C}$  and time of 4 h (Fig. 9a) has a similar depth as the layer nitrided in the same variant but at a higher temperature ( $400^\circ\text{C}$ ). However, intensity of the diffraction reflections from the surface layer nitrided in lower temperature shows that there are less nitride phases and nitrogen saturated austenite. The diffraction patterns from the cathode-nitrided layers show that there is a further decrease of  $\text{CrN}$ ,  $\text{Cr}_2\text{N}$  and  $\gamma\text{N}$  phases.

Diffraction patterns of X2CrNiMo17-12-2 steel nitrided with the use of an active screen at temperature of  $325^\circ\text{C}$  and time of 2 h (Fig. 11a) show weak outlines of the peaks coming from nitride phases and nitrogen saturated austenite. It speaks for the fact that these phases have a small participation in the subsurface zone. Reflection coming from the nitrogen saturated austenite is partially imposed upon the peak from austenite  $(111)\gamma$ , which means that there is a small nitrogen saturation. The diffraction pattern of the cathode-nitrided layer at the same parameters (Fig. 12a), at the smallest angles of incidence shows that there are peaks coming from a subtly nitrogen saturated austenite. However, reflections from the nitrides did not appear. The peaks from the nitrides can be observed in XRD analyses (Fig. 12b).

The depths of the obtained nitrided layers calculated with the help of GIXRD method are estimated values and can be error-burdened. It follows from the assumptions concerning  $G_x$  parameter, which values are not determined clearly in literature and should be selected individually. The obtained results can be used for overall analyses, and the obtained values should be verified by comparing them with the results obtained by other methods.

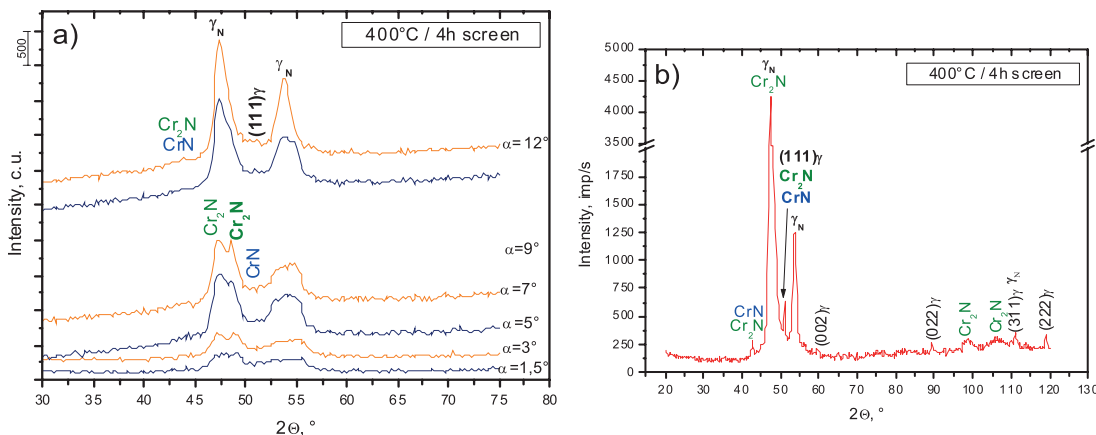


Fig. 5. Diffraction patterns of the layer nitrided with the use of an active screen at temperature of  $400^\circ\text{C}$  and time of 4 h obtained: a) by GIXRD method; b) by XRD method

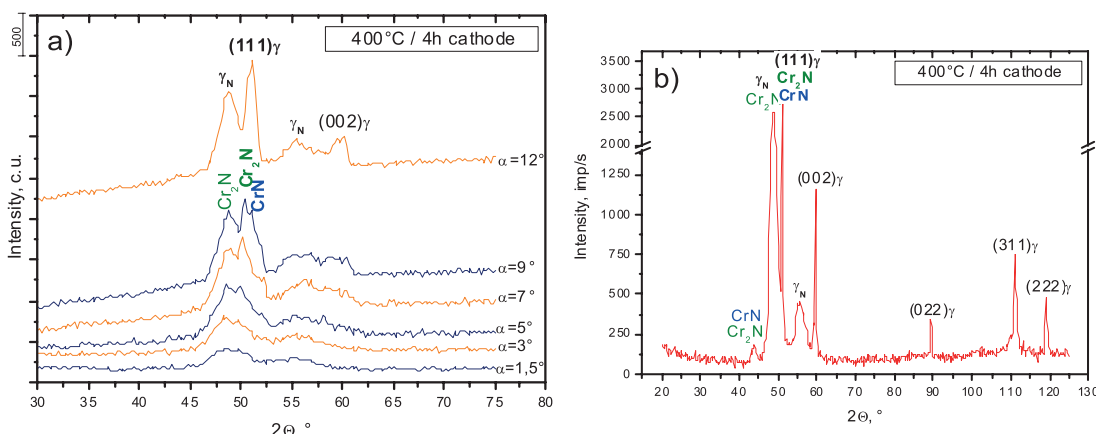


Fig. 6. Diffraction patterns of the cathode-nitrided layer at temperature of  $400^\circ\text{C}$  and time of 4 h obtained: a) by GIXRD method; b) by XRD method

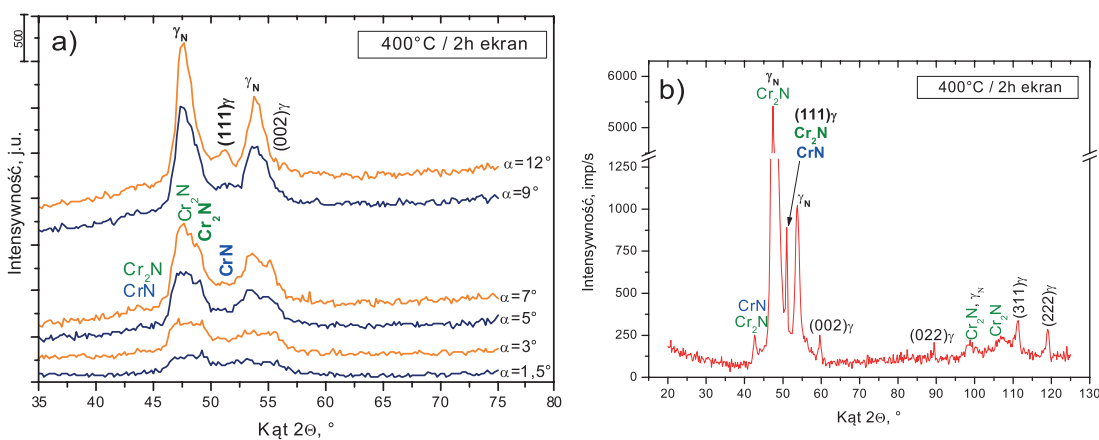


Fig. 7. Diffraction patterns of the layer nitrided with the use of an active screen at temperature of 400°C and time of 2 h obtained: a) by GIXRD method; b) by XRD method

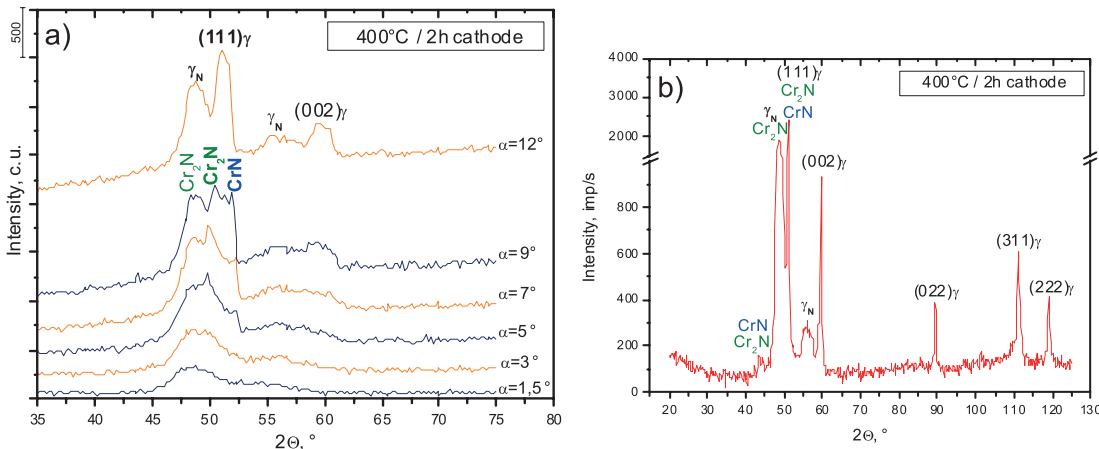


Fig. 8. Diffraction patterns of the cathode-nitrided layer at temperature of 400°C and time of 2 h obtained: a) by GIXRD method; b) by XRD method

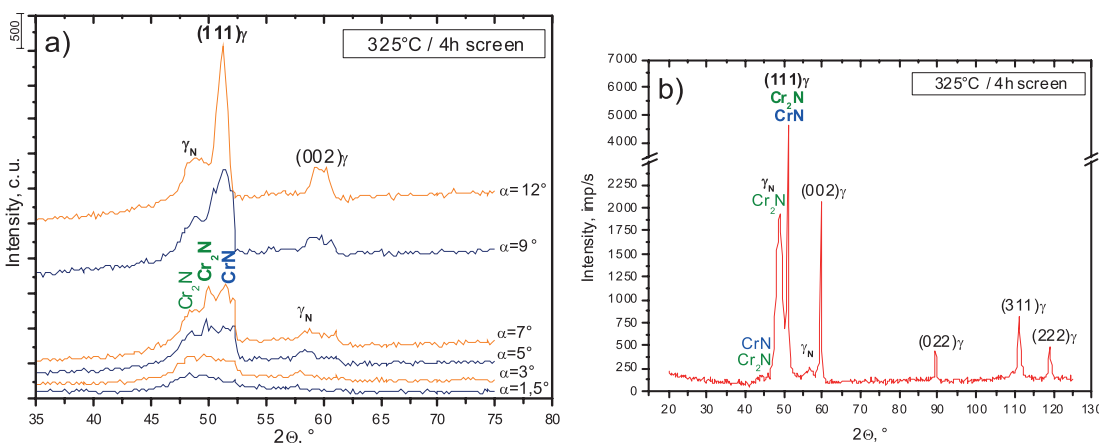


Fig. 9. Diffraction patterns of the layer nitrided with the use of an active screen at temperature of 325°C and time of 4 h obtained: a) by GIXRD method; b) by XRD method

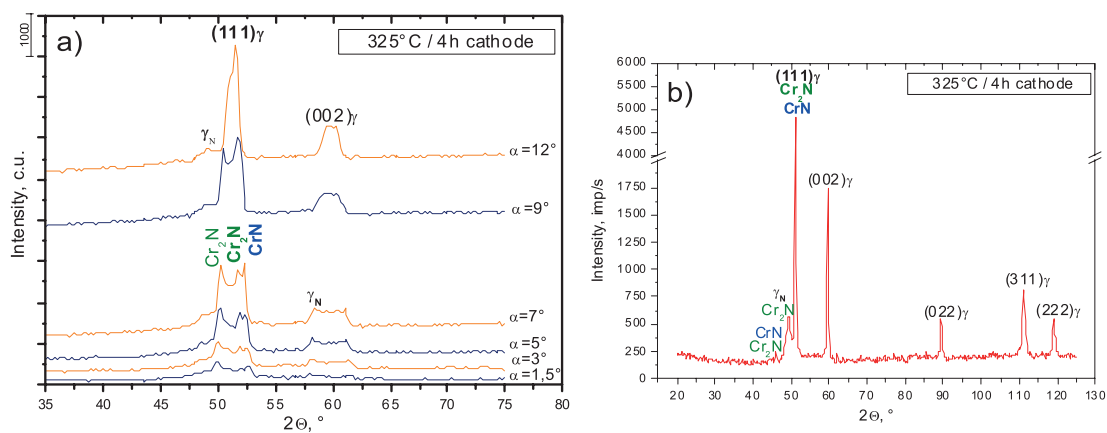


Fig. 10. Diffraction patterns of the cathode-nitrided layer at temperature of 325°C and time of 4 h obtained: a) by GIXRD method; b) by XRD method

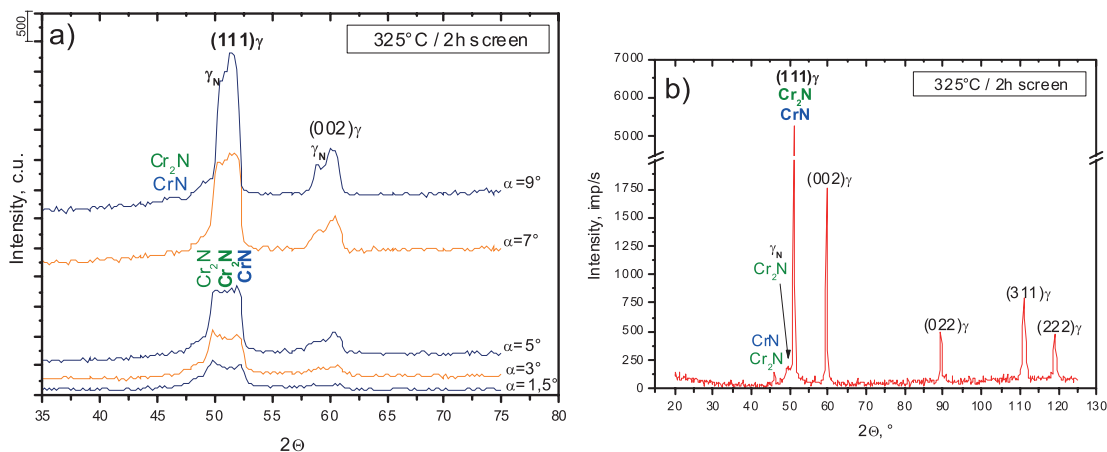


Fig. 11. Diffraction patterns of the layer nitrided with the use of an active screen at temperature of 325°C and time of 2 h obtained: a) by GIXRD method; b) by XRD method

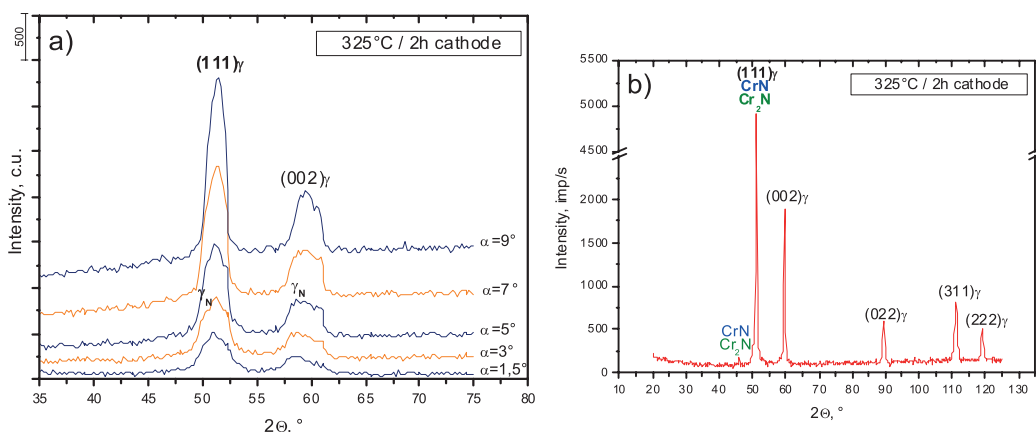


Fig. 12. Diffraction patterns of the cathode-nitrided layer at temperature of 325°C and time of 2h obtained: a) by GIXRD method; b) by XRD method

#### 4. Conclusions

On the basis of the carried out analysis it was stated that the use of an active screen intensifies a plasma nitriding process. As a result, obtained a nitride layer of increased thickness in comparison to a similar cathode process. The GIXRD analyses showed the presence of the peaks coming from chromium nitrides, which were especially intensive at the smallest angles of incidence of X-rays, close to the surface areas. The decrease of time and temperature of the process on the diffractive areas caused a significant drop of intensity of the peaks coming from the nitride phases and simultaneous increase of reflections coming from the base. On the basis of the X-ray analyses it was stated that the analyzed layers have a zone structure. They respectively consist of a subsurface zone of chromium nitrides and a zone of nitrogen saturated austenite.

#### REFERENCES

- [1] T. Budzynowski, Ocena wpływu azotowania na kształtowanie wybranych właściwości użytkowych staliw stopowych, Politechnika Radomska, Radom (2009).
- [2] M. Esfandiari, H. Dong, Improving the Surface Properties of A286 Precipitation-Hardening Stainless Steel by Low-Temperature Plasma Nitriding, *Surf. Coat. Technol.* **201**, 6189-6196 (2007).
- [3] J. Baranowska, W. Serwiński, A. Zieliński, Obróbka powierzchniowa nierdzewnej stali austenitycznej, *Inżynieria Materiałowa* **5**, 279-281 (1999).
- [4] B. Kucharska, Measurement of Fe-Cr-Ni coating density in XRD analysis, *Inżynieria Materiałowa* **3 – 4**, 419-421 (2007).
- [5] P. Colombi, P. Zanola, E. Bontempi, L.E. Depero, Modeling of glancing incidence X-ray for depth profiling of thin layers, *Spectrochimica Acta Part B* **62**, 554–557 (2007).
- [6] T. Frączek, M. Olejnik, J. Jasiński, Z. Skuza, Short-Term, Low Temperature Glow Discharge Nitriding of High-Chromium X2CrNiMo17-12-2 Steel, *Metallurgy* **49**, 3, 151-154 (2010).
- [7] M. Olejnik, T. Frączek, Analiza fazowa warstw azotowanych na podłożu stali austenitycznej X2CrNiMo17-12-2, *Hutnik-Wiadomości Hutnicze* Vol. 78, nr 9, 757-760, (2011).
- [8] S. Kłysz, A. Bień, Badania struktury i mikrotwardości warstwy konstytuowanej laserowo na stali konstrukcyjnej, *Prace Naukowe ITWL* **23**, 37-49 (2008).

Received: 20 Marz 2015.